

EROSION-CORROSION BEHAVIOR OF AA 6066 ALUMINUM ALLOY

OSAMA ERFAN¹, AL-BADRAWY ABO EL-NASR² & FAHAD AL-MUFADI³

^{1,3}Department of Mechanical Engineering, College of Engineering, Qassim University, KSA

²Department of Production Engineering and Mechanical Design, Faculty of Engineering,
Menoufiya University, Shebin El-Kom, Egypt

¹Department of Production Engineering, Beni Swef University, Beni Swef, Egypt

ABSTRACT

Erosion-Corrosion (E-C) behavior of AA 6066 aluminum alloy has been studied in two different environments namely; 3.5 wt.% NaCl solution and 3.5 wt.% NaCl solution contains 20 wt.% sand particles. E-C tests were carried out using a test rig designed particularly for this purpose. The tests aims to study the effect of testing time, flow velocity, the projected area and impact angle on the E-C behavior of the alloy. The eroded–corroded surfaces were examined using scanning electron microscopic (SEM) to elucidate the mechanism of material removal.

The obtained results indicate that the weight-loss increased with increasing testing time, flow velocity and the projected area due to the increase in the severity of erosive/abrasive attacks. While for impact angle, as it increased from 15° up to 90°, the weight-loss decreased. SEM observations of E-C surfaces exhibited that an increase in the testing time leads to uniform pits formation that accommodated and covered the whole surface, resulting in an increase in their size. It is observed that erosion process is the dominant mode of material removal in the present E-C environment.

KEYWORDS: Erosion- Corrosion, AA 6066, NaCl Solution, Sand Particles, Pits, Weight-Loss

INTRODUCTION

Erosion-Corrosion (E-C) is a degradation of material surface due to mechanical action, often by impinging liquid, abrasion by a slurry, particles suspended in fast flowing liquid or gas, bubbles, cavitations, ... etc [1,2]. E-C is associated with a flow-induced mechanical removal of the protective surface film that results in a subsequent corrosion rate increase via either electrochemical or chemical processes. The existence of such a phenomenon accelerates the corrosion attack in the metal surface due to the relative motion of a corrosive fluid on the exposed surface. The interactions between these two processes are complex in nature where both processes can either complement each other in accelerating the total wear rate of a material or in certain cases suppress the total wear rate [3]. E-C related problems occur in power plants, oil and gas processing plants and chemical plants where there is an interaction between solid particles, corrosive fluid and a target material. It usually results in corrosion that occurs at a higher rate than would be expected under stagnant conditions. The problem has been, also, reported to affect static equipment for example pipelines, valves, heat exchangers and pressure vessels. The importance of material selection for applications in these environments cannot be overstated as component wear can be accelerated by the aggressive conditions in these harsh environments [4].

Several investigations have been conducted to understand the effects of various variables on E-C of some engineering materials [4-11]. For example, Niu and Cheng [10,11] investigated the effects of fluid hydrodynamics on Al alloy corrosion in ethylene glycol-water solutions by using rotating disc electrode (RDE) technique. It was found that, in the absence of sands, Al alloy corrosion is dominated by the oxygen diffusion towards the electrode surface. It was

generally found that the total weight-loss of materials in E-C media is much higher than those caused by pure corrosion or pure erosion individually [12-14]. Studies of E-C behavior of MMCs and their matrices are limited [15-17]. In order to determine the total wear rate caused by the combined effect of erosion and corrosion, various test rigs have been designed. Among these test rigs are slurry pot erosion tester [4,20,21], jet impingement test rig [4-6, 20,21], Coriolis erosion tester [17], pipe flow loop [10,11] and rotating cylinder apparatus [5,12,15]. Each of these test rigs has its advantages and disadvantages in terms of ease of usage and ease of maintenance, cost and control of test parameters.

Two mechanisms were suggested for the explanation of E-C interaction behavior [18,19]. The former is the corrosion-enhanced erosion which is related to the degradation of surface hardness or strength of materials. The role of corrosion is to roughen the material surface, which in turn greatly increases the erosion rate. The later is the erosion-enhanced corrosion which is caused by the retardation of formation of a protective film on metal surface. As a consequence, corrosion proceeds at a high rate in the absence of such protective films. Furthermore, pitting phenomenon has been observed during E-C investigations [21-23]. Burstein and Sasaki [22] studied the initiation of corrosion pits by slurry erosion on stainless steel and found that below a pitting potential, slurry erosion causes formation of more metastable pits compared to non-erosive conditions. This was attributed to the rupture and removal of the passive film by solid particle impacts. Surface roughness was also suggested to have an effect on pitting potential [23]. Rougher surfaces as a result of slurry erosion, lowers the pitting potential hence increases its susceptibility to form pits.

This work aims to investigate E-C behavior of AA 6066 aluminum alloy through series of experiments for measuring the weight-loss in addition to surface inspection. Parameters under consideration include; testing time, flow velocity, the projected area to the flow and impact angle. SEM examinations were also conducted to elucidate the mechanism that may control E-C behavior of the present alloy.

EXPERIMENTAL WORK

Material and Specimens

The material used in this work was an aluminum alloy namely; AA 6066 aluminum. The chemical composition of the alloy is given in Table 1 and the basic mechanical properties of the alloy are: $\sigma_{UTS} = 150$ MPa, $\sigma_Y = 83$ MPa, $E = 80$ GPa. The importance of 6xxx alloys came from the progressive increase in using them as matrices for metal matrix composites (MMCs), replacing conventional materials due to their high thermal conductivity, excellent formability and relatively good corrosion resistance [15]. The alloy was received in as-extruded rods. Sets of finger-shaped specimens were cut to a diameter of 12 mm and 60 mm as a length, as specified in ASTM standard [24]. Other groups of the specimens with different diameters and lengths are also used. Prior testing, the specimens were polished using standard metallographic techniques ensuring that no scratches existed on the surface and the average roughness of the specimens surfaces was found to be about $R_a = 0.62 \pm 0.06$ μm .

Table 1: Chemical Composition of AA 6066 Aluminum Alloy Used in the Present Work

Element	Si	Fe	Cu	Mn	Mg	Cr	Zn	Ti	Al
Wt. %	1.3	0.5	1.0	1.0	1.2	0.25	0.2	0.1	Balance

Erosion-Corrosion Tests

E-C tests were carried out using the rotating specimen method in a saline abrasion media. The test rig, used in this work, consists mainly of a drill machine that was modified and adapted to fit the present experiments as shown schematically in Figure 1a. The tests were conducted for specimens of AA 6066 alloy in two different media, namely 3.5 wt.% NaCl solution and 3.5 wt.% NaCl solution containing 20 wt.% of sand particles. Natural uncrushed silica

with specific size $205\pm 40\ \mu\text{m}$ was used as erosive elements. The rotational speed was remained constant over the whole tests, 1200 rpm. A thermo-set plastic circular disc was designed and manufactured for mounting the test specimens. An optical photo of the disc as well as the test specimens are shown in Figure 1b. As seen, the specimens were mounted with respect to the fluid motion in such a way that they receive normal impact from the sand particles during their rotation. The disc is equipped with a shaft at its center to be mounted with the spindle of the test machine.

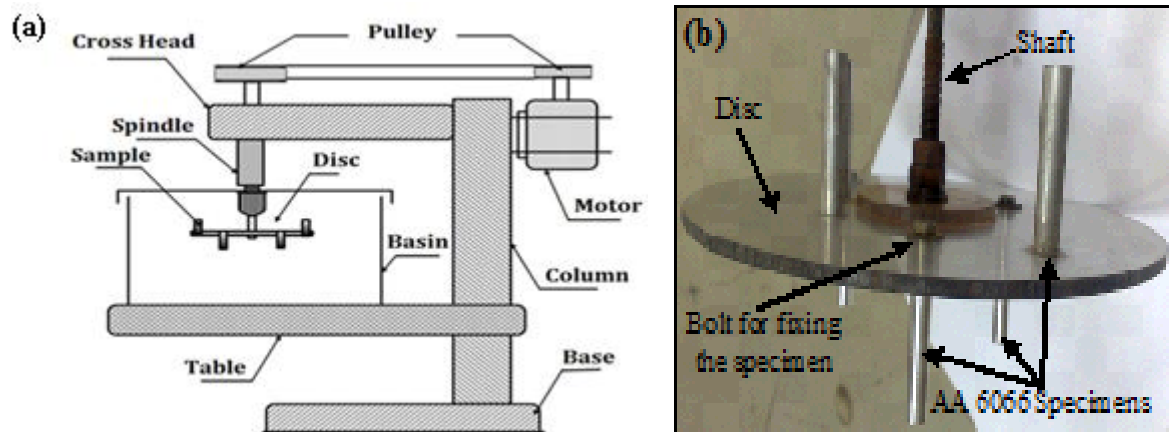


Figure 1: a) A Schematic Draw of the Test Rig Used in the Present Study and b) Optical Photo of the Polymeric Disc Used for Fixing the Test Specimens

Series of E-C tests were conducted to measure the effect of testing time, flow velocity, the projected area and impact angle on the weight-loss of material used. Tests were conducted at different flow velocities ranged between 1 to 3 m/s. To measure the effect of impact angle of impinging sand particles on the specimen surface, the tests were performed by making the samples to be inclined with different angles starting from 15° up to 90° . Weight-loss per unit area was computed to measure the E-C rate by weighting the test specimens before and after testing, using a high sensitive digital balance with a precision of 0.1 mg. Prior testing, the specimens were polished using standard metallographic techniques and mounted on the disc at a different radial distances in order to get different linear velocities. A polymeric basin was used as a container of the saline solution. Measurements were repeated at least 3 times for each test and the average of weight-loss was reported.

SEM Examination

Scanning Electron Microscopy (SEM) (JEOL-JSM-6510LV) was used to examine the eroded-corroded surfaces. SEM examinations were performed for specimens tested for four testing times; 12, 24, 36, and 48 hrs. Prior investigations, the specimens were cleaned by a stream of clean water and air under pressure.

RESULTS AND DISCUSSIONS

Influence of Testing Time on E-C Behavior

Figure 2 shows the results of E-C tests of specimens of AA 6066 alloy as a weight-loss vs testing time in 3.5 wt.% NaCl solution and in 3.5 wt.% NaCl solution containing 20 wt.% sand particles at three different flow velocities; 1.5, 2 and 3 m/s, respectively. The weight-loss is used herein to represent the wear rate due to E-C effects on the present alloy. As shown in Figure 2a, for a flow velocity of 1.5 m/s and NaCl solution, the weight-loss increased from $0.0 \times 10^{-6}\ \text{gm/mm}^2$ at 3 hrs to $\sim 1.2 \times 10^{-6}\ \text{gm/mm}^2$ at 36 hrs, while in a water solution contains both NaCl and 20 wt.% sand particles, the weight-loss increased from $\sim 0.4 \times 10^{-6}\ \text{gm/mm}^2$ at 3 hrs to $\sim 1.6 \times 10^{-6}\ \text{gm/mm}^2$ at 36 hrs. Figure 2b shows the relationship between weight-loss per unit area and time for a flow velocity of 2 m/s. It is noticed that for the solution containing only NaCl, as indicated on the right axis, the weight-loss increased from $\sim 0.15 \times 10^{-6}\ \text{gm/mm}^2$ at 3 hrs

to $\sim 1.2 \times 10^{-6}$ gm/mm² at 36 hrs while for a water solution containing both NaCl and 20 wt.% sand particles, the weight-loss increased from $\sim 13 \times 10^{-6}$ gm/mm² at 3 hrs to $\sim 90 \times 10^{-6}$ gm/mm² at 36 hrs. Figure 2.c shows for a velocity of 3 m/s in case of the NaCl solution that the weight-loss increased from $\sim 0.4 \times 10^{-6}$ gm/mm² to $\sim 2.5 \times 10^{-6}$ gm/mm², while for NaCl solution containing 20 wt.% sand particles, the weight-loss increased from $\sim 20 \times 10^{-6}$ gm/mm² to $\sim 170 \times 10^{-6}$ gm/mm² at 36 hrs. It is evident from these results that similar trends are obtained for the alloy where the weight-loss increases with increasing the testing time for different flow velocities. Another finding that AA 6066 alloy exhibited less E-C resistance due to the existence of sand particles in NaCl solution (E-C effects) compared to that tested only in NaCl solution, corrosion type. In a comparison among these results, the influence of velocity on the E-C behavior is clearly evident.

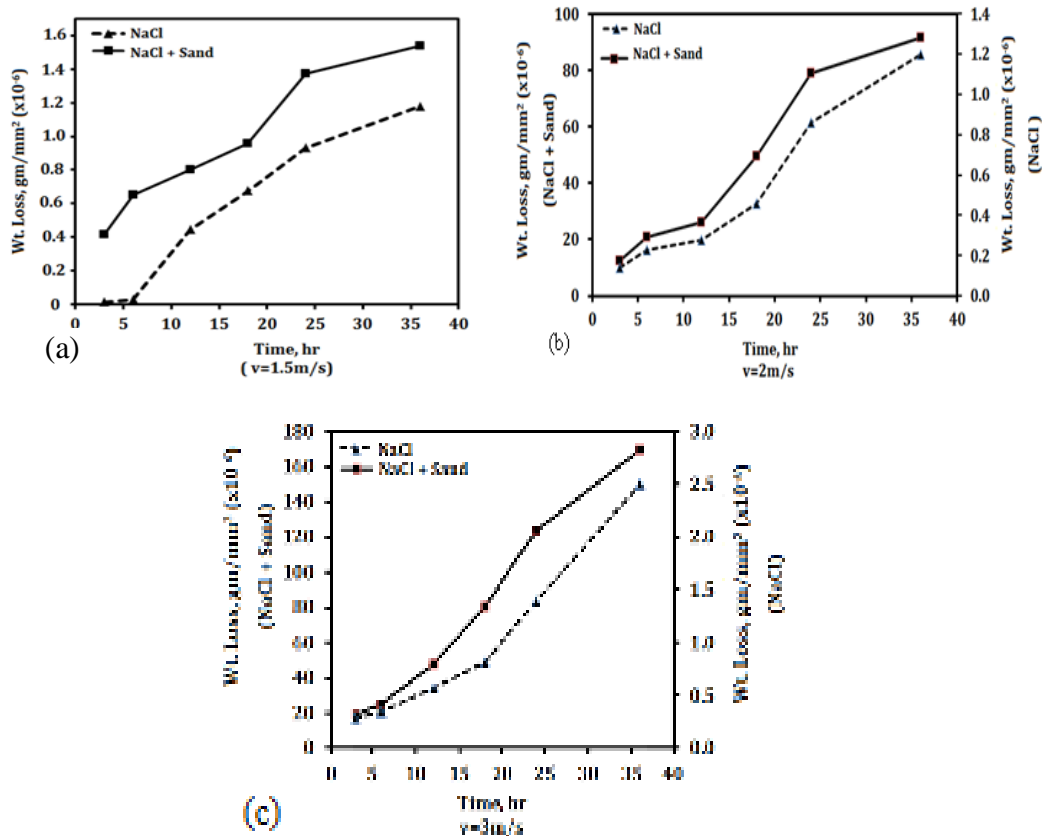


Figure 2: Weight-Loss vs Testing Time for AA 6066 Alloy Tested in NaCl Solution and NaCl Solution with 20 wt.% Sand Particles; a) Velocity: 1.5 m/s, b) Velocity: 2 m/s and c) Velocity: 3 m/s

Influence of Flow Velocity on E-C Behavior

Figure 3 shows the weight-loss per unit area vs the flow velocity for specimens of AA 6066 alloy. It is observed that for NaCl solution, the weight-loss increased from $\sim 0.5 \times 10^{-6}$ gm/mm² at a velocity 1 m/s to $\sim 1.5 \times 10^{-6}$ gm/mm² at a velocity 3 m/s while for NaCl solution containing sand particles, the weight-loss increased from $\sim 18 \times 10^{-3}$ at a velocity 1 m/s to $\sim 140 \times 10^{-3}$ gm/mm² at a velocity 3 m/s, the right axis. The graph shows that the weight-loss, as in case of NaCl solution that contains sand particles (E-C media), is greater than that for the case of NaCl solution (corrosion type). This increase in weight-loss may be attributed to the increase in severity of the erosive/corrosive attack as the velocity increased. It is expected that the mechanism that may drive the E-C behavior in such a case is a mechanical erosion of the material of the formed oxide layer on the surfaces and enhanced corrosion of the material.

Influence of the Projected Area on E-C Behavior

Figure 4 shows the weight-loss per unit area vs the projected area of specimens of AA 6066 alloy that exposed to normal impact of sand particles in NaCl solution. For the specimens tested in NaCl solution, with increasing the projected area, the weight-loss increased from $\sim 18 \times 10^{-6}$ to $\sim 85 \times 10^{-6}$ gm/mm². For the specimens tested in NaCl solution that contains sand particles, the weight-loss increased from $\sim 18 \times 10^{-6}$ to $\sim 110 \times 10^{-6}$ gm/mm² in the same range of projected areas. As shown in this figure, in the low value of projected area the value of the material removal, for both two media, are closely equals and as the projected area increased the effect of E-C increased compared to that tested in NaCl solution only. It is noted from the present results that the wear rates increased with increasing the exposed area to E-C media due to increase in the severity of erosive/abrasive attacks. These findings are in consistent with the previous results that came to a conclusion that the role played by mechanical erosion and enhanced corrosion is the main reason of the material removal.

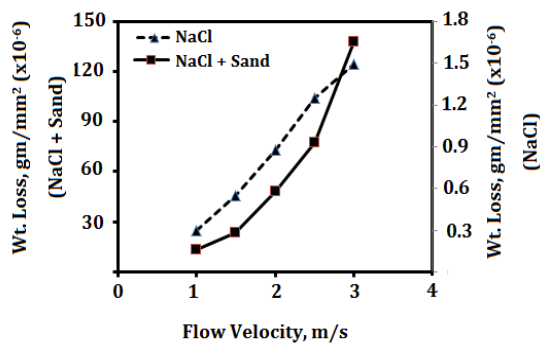


Figure 3: Weight-Loss vs Flow Velocity of Specimens of AA 6066 Alloy. All Specimens Were Tested for 24 Hrs and a Velocity 2 m/s

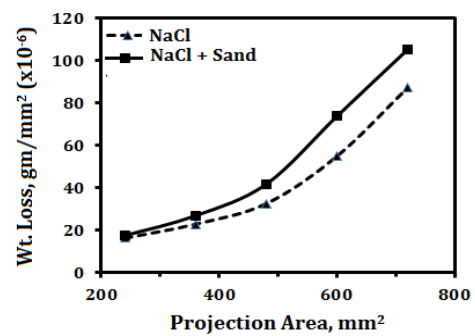


Figure 4: Weight-Loss vs the Projected Areas of Specimens of AA 6066 Alloy. All Specimens Were Tested for 24 Hrs and a Velocity 2 m/s

Influence of Impact Angle on E-C Behavior

Figure 5 shows the effect of the impact angle on the weight-loss per unit area in E-C media. As shown in the figure, increasing the impact angle resulted in decreasing the weight-loss values. In case of using NaCl solution, the weight-loss is almost constant with varying the impact angle from 15° to 90°. On the other hand, in case of E-C tests, the weight-loss decreased from $\sim 200 \times 10^{-6}$ gm/mm² to $\sim 120 \times 10^{-6}$ gm/mm². The effect of the impact angle on E-C behavior of the alloy is dependent on the distribution of shear stress and normal stress exerting on the specimen surface. Whenever the specimen is subjected to normal impact of sand particles, the shear force, due to rolling of erodent particles on the specimen surface, causes minimum damage and consequently material removal due to abrasion in minimized [17]. With the decrease of impact angle, shear stress becomes dominant and resulting in an increasing E-C rate. It is believed that erosion has played the dominant component in material removal of E-C of the alloy.

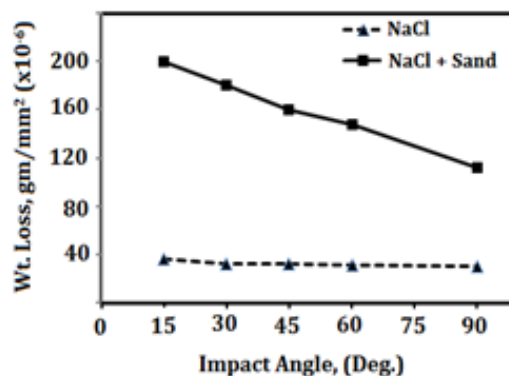


Figure 5: Weight-Loss per Unit Area vs Impact Angle for Specimens of AA 6066 Alloy Tested for 24 Hrs in NaCl Solution with 20 wt. % Sand Particles, and Flow Velocity of 2 m/s

SEM Observations

Figure 6 shows SEM micrographs of the surface topography of specimens of AA 6066 alloy tested in E-C media for different testing times namely; 12, 24, 36 and 48 hrs. The micrographs show a typical pitting process caused by NaCl solution containing 20 wt.% sand particles which is able to hit and penetrate the surface. It is obvious from these micrographs that grooves and pits were formed on the surface along with the fluid impact. It is seen from these micrographs that as the testing time increased the number of the pits increased and grooves size tends to vanish. For example, in case of 12 hrs testing time, in Figure 6.a, grooves with a little number of fine pits were observed uniformly distributed on the specimen surface. For a longer testing time, 48 hrs, the specimen surface was dominated by a large number of pits and the grooves were decreased. Figure 7.a and b shows two images of the eroded-corroded surfaces for the periods of 36 and 48 hrs with a higher magnification. As shown, the testing time has played a significant role in determining the nature of final surface of these specimens. It is believed for longer time that the number of metastable pits formed leading to a higher probability of reaching stable pits is also increased.

These observations are in agreement with a severe regime of corrosion-affected erosion, in which the damage includes both the oxides and the base metal. This finding is supported by the measurement of the average size of the pits in Figure 8 in which as the testing time increased the average size of the pits is increased. For the specimen tested for 12 hrs, the average size of pits is $1.15 \mu\text{m}$ and for the specimen tested for 48 hrs, the average size of pits is $2.35 \mu\text{m}$. When the sand particles collide with the surface of the samples, this collision converts kinetic energy of the sand particles into potential energy, which makes the surface layer of the specimens is gaining elastic strain energy. Erosion mechanism of AA 6066 alloy by eroding sand particles in a fluid involves deformation on the exposed surface due to slip band formation as a result of mechanical action caused by the transferred kinetic energy to the surface [24].

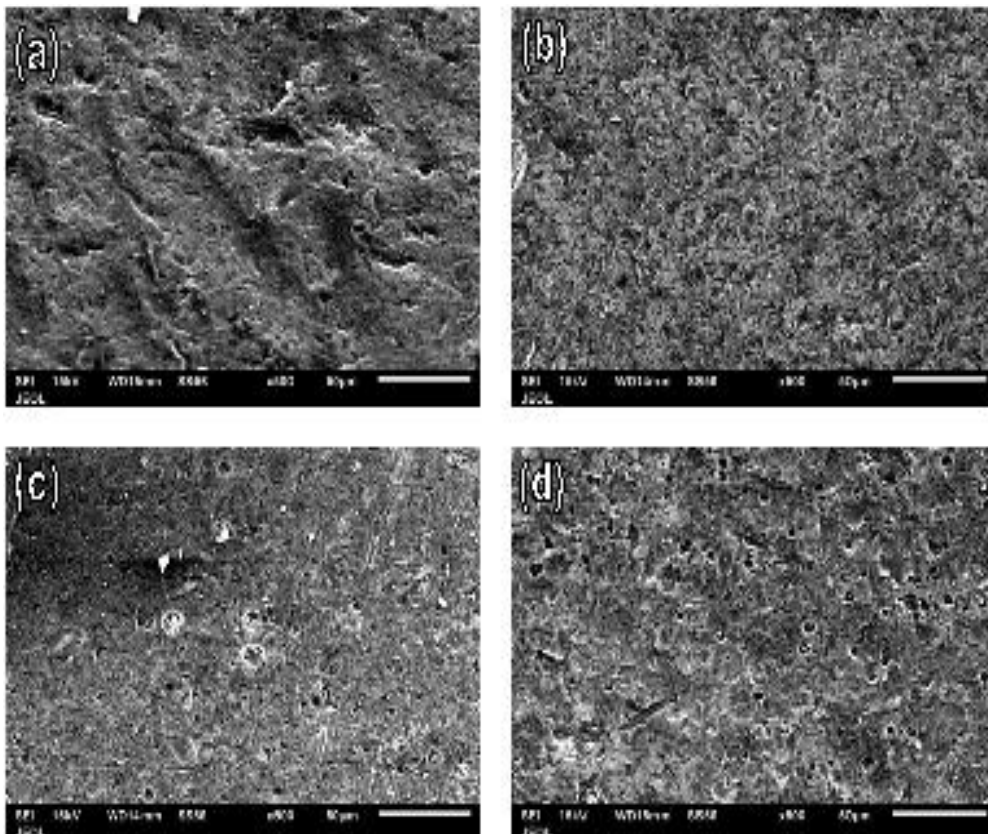


Figure 6: SEM Micrographs of Eroded-Corroded Surfaces of Specimens of AA 6066 Alloy Under Different Testing Times (x500); (a) for 12 Hrs, (b) for 24 Hrs, (c) for 36 Hrs, and (d) for 48 Hrs

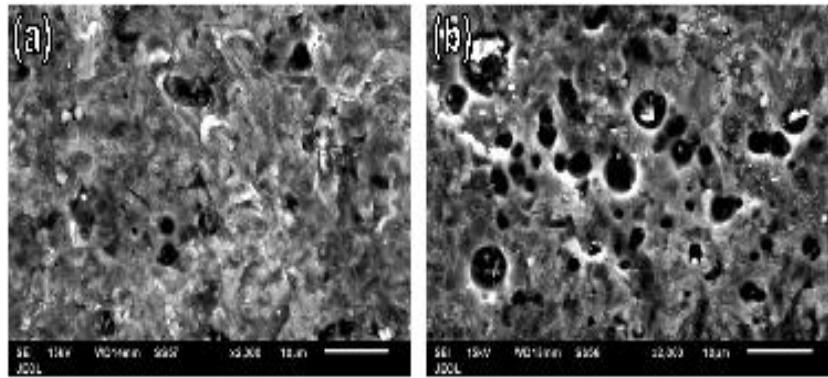


Figure 7: Typical SEM Micrographs of Eroded-Corroded Surface of Specimens of AA 6066 Alloy, at High Magnification (x2000); (a) Tested for 36 Hrs and (b) Tested for 48

E-C Mechanism

The present findings exhibited that the interaction between the basic processes of erosion and corrosion is complex, but can be rationalized into a series of regimes with a smooth transition from one regime to the next as the relative intensity of one process is varied with respect to the other. The type of interaction between erosion and corrosion apparently depends on the oxides formed in terms of their initiation and rate of growth and the media used. The dominant mechanism may change based on the interaction by changing the conditions. In the case of the present alloy, a change of regime could occur with extending the time of exposure as the composition of the alloy surface and the mode of oxidation change. The erosion damage to the surface layers apparently allowed the oxidants to penetrate and produce internal attack of the metal. This confirms the important role of oxide formation in the E-C mechanism. The formation of an oxide layer that can withstand the impact of erosion has been found to provide some protection. Due to the presence of sand particles in NaCl solution, the erosive and abrasive actions of the particles removed the corrosion products, exposing new surfaces. It is suggested that the oxide film suffers brittle erosion at the impact sites, where oxidation resumes, leading to stepped increases in oxidation rate at the individual sites and a substantially increased rate of attack. This may explain the observation that the formed pits were bigger than those formed with specimens tested for shorter time. It is also possible that the presence of erosion in some way enhanced the growth rate of the pits.

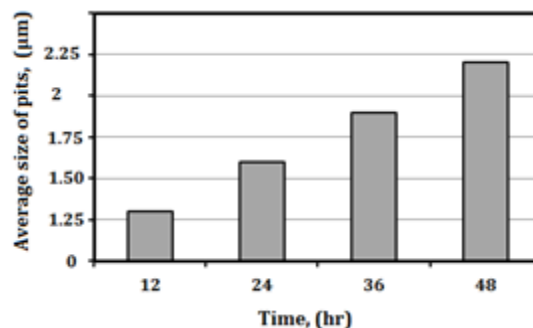


Figure 8: Histogram of the Average Size of Surface Pits vs Testing Time that Formed After E-C Tests for AA 6066 Alloy

It is well established that whenever a metallic alloy is exposed to an erosive-corrosive media, it generally experiences material removal on the surface layer due to corrosion by the solution and erosion by the impinging action of liquid droplets formed by the turbulent flow in addition to the interaction between them [25,26]. The total wear rate due to E-C effects, W_T , can be expressed by the following expression:

$$W_T = W_C + W_E + W_M \quad (1)$$

where W_C is the pure corrosion rate in the absence of erosion effect, W_E is the pure erosion rate in the absence of corrosion effect and W_M represents the mutual effect between erosion and corrosion. The mutual effect represents the additive effect due to erosion-enhanced corrosion rate, W_{CE} , in addition to synergistic effect due to corrosion-enhanced erosion rate, W_{EC} . On the basis of this, Eq. 1 can be rewritten as follow:

$$W_T = W_C + W_E + (W_{CE} + W_{EC}) \quad (2)$$

This relationship may formulate the thought that, in the E-C media, four components affect the alloy surface. The first term relates to the individual effect due to corrosion. The second term relates to the individual effect due to erosion. The third term relates to interrelated effect the additive effect due to erosion-enhanced corrosion rate. The last one relates to the synergistic effect due to corrosion-enhanced erosion rate. However, the mechanism of the interaction of erosion and corrosion on the surface of the alloy in saline containing sands particles is still needs more investigations to find out the mechanism that controls this interaction.

CONCLUSIONS

On the basis of the obtained results and accompanying discussion of E-C behavior of AA 6066 alloy tested in two environments; 3.5 wt.% NaCl water solution and 3.5 wt.% NaCl water solution containing 20 wt.% sand particles, the following conclusions can be made:

- The weight-loss of the alloy increases with increasing the testing time, flow velocity and the projected area. Meanwhile, the total weight-loss in case of NaCl solution that contains sand particles (E-C media) is generally higher than that caused by NaCl solution (corrosion type). This behavior may be attributed basically to the increase in the severity of erosive/abrasive attacks and the synergistic effects of mechanical wear and chemical attack. The the weight-loss also decreases with the increase on impact angle. With the decrease of impact angle, shear stress becomes dominant and resulting in an increase E-C rate and erosive attack was expected to be the dominant mode of material removal.
- The interaction between the basic processes of erosion and corrosion can be rationalized into a series of regimes with a smooth transition from one regime to the next as the relative intensity of one process is varied with respect to the other. Erosion process is the dominant mode of material removal in low testing time. Erosion mechanism of AA 6066 alloy may involve deformation on the exposed surface as a result of mechanical action caused by the transferred kinetic energy to the surface.
- E-C attack in the alloy occurred by the formation of surface pits at those sites that were strongly influenced. The results show that the contribution of corrosion is minor and erosion component is the dominant part. The testing time has played a significant role in determining the feature of the final surface of the specimens. It is believed for longer testing time that large number of metastable pits formed leading to a higher probability of reaching stable pits.

REFERENCES

1. Z. Kamid, P.H. Shipway, T. Voisey, A.J. Sturgeon, "Abrasive wear behavior of conventional and large particle tungsten carbide-based cement coatings as a function of abrasive size and type", *Wear* 271, (2011), pp. 1264-1272.

2. E. A. M. Hussain, M. J. Robinson, "Erosion-corrosion of 2205 duplex stainless steel in flowing seawater containing sand particles", *Corrosion Sci.* 49, (2007), pp. 1737-1744.
3. I. M. Hutchings, "Tribology-Friction and wear of engineering materials", Edward Arnold, (1992).
4. S. S. Rajahram, T.J. Harvey, R.J.K. Wood, "Erosion-corrosion resistance of engineering materials in various test conditions", *Wear* 267, (2009), pp. 244-254.
5. G. T. Burstein, K. Sasaki, "Effect of impact angle on slurry erosion-corrosion of 304 L stainless steel", *Wear* 240, (2000), pp. 80-94.
6. B. D. Jana, M.M. Stack, "Modeling impact angle effects on erosion-corrosion of pure metals: construction of materials performance maps", *Wear* 259, (2005), pp. 243-255.
7. B. Thirumaran, S. Natarajan, S. P. Kumaresh, "Corrosion behavior of CNT reinforced AA 7075 Nanocomposites", *Advances in Mater*, 2 (1), 2013, pp. 1-5.
8. H. Meng, X. Hu, A. Neville, "A systematic erosion-corrosion study of two stainless steels in marine conditions *via* experimental design", *Wear* 263, (2007), pp. 355-362.
9. G. A. Zhang, L.Y. Xu, Y.F. Cheng, "Investigation of erosion-corrosion of 3003 aluminum alloy in ethylene glycol-water solution by impingement jet system", *Corrosion Sci.* 51, (2009), pp. 283-290.
10. L. Niu and Y. F. Cheng, "Electrochemical characterization of metastable pitting of 3003 aluminum alloy in ethylene glycol-water solution", *J Mater Sci*, 42 (2007), pp. 8613-8617.
11. L. Niu, Y.F. Cheng, "Erosion-corrosion of aluminum alloy in ethylene glycol-water solutions in the absence and presence of sand particles", *Corrosion Eng. Sci. Tech.* 44 (2009), pp. 389-393.
12. V. A. D. Souza, A. Neville, "Aspects of microstructure on the synergy and overall material loss of thermal spray coatings in erosion-corrosion environments", *Wear* 263, (2007), pp. 339-346.
13. Y. Li, G. T. Burstein, I.M. Hutchings, "The influence of corrosion on the erosion of aluminum by aqueous silica slurries", *Wear* 186-187 (1995), pp. 515-516.
14. S. S. Rajahram, T.J. Harvey, R.J.K. Wood, "Evaluation of a semi-empirical model in predicting erosion-corrosion", *Wear* 267 (2009), pp. 1883-1893.
15. W. S. Miller, L. Zhuang, J. Bottema, A.J. Wittebrood, P. De Smet, A. Haszler, A. Viergege, "Recent development in aluminium alloys for the automotive industry". *Mater Sci Eng, A* 280, (2000), pp. 37-49.
16. B. K. Prasad, "Wear characteristics of a zinc-based alloy compared with a conventional bearing bronze under lubrication conditions: Effects of material and test parameters", *Wear* 238 (2), (2000), pp. 151-159.
17. S. Das, D. P. Mondal, O. P. Modi, and R. Dasgupta, "Influence of experimental parameters on the erosive-corrosive wear of Al-SiC particle composite", *Wear* 231 (2), (1999), pp. 195-205.
18. Y. Liu, Y.F. Cheng, "Inhibition of corrosion of 3003 aluminum alloy in ethylene glycol-water solution", *J Mater Eng Perfor* 20, (2011), pp. 271-275.
19. M. M. Stack, T.M. Abd-El Badia, "Mapping erosion-corrosion of WC/Co-Cr based composite coatings: particle velocity and applied potential effects", *Surface and Coatings Tech*, 201 (2006), pp. 1335-1347.

20. G. C. Liang, X.Y. Peng, L.Y. Xu, Y.F. Cheng, "Erosion-corrosion of carbon steel pipes in oil sands slurry studied by weight-loss testing and CFD simulation", *J Mater Eng Perfor*, accepted on Apr. 29, 2013
21. Y. Yang, Y.F. Cheng, "Parametric effects on the erosion-corrosion rate and mechanism of carbon steel pipes in oil sands slurry", *Wear* 276-277 (2012), pp. 141-148.
22. G. T. Burstein, K. Sasaki, "The birth of corrosion pits as stimulated by slurry erosion", *Corrosion Sci*, 42, (2000), pp. 841-860.
23. K. Sasaki, G. T. Burstein, "The generation of surface roughness during slurry erosion-corrosion and its effect on the pitting potential", *Corrosion Sci* 38 (12) (1996), pp. 2111-2120.
24. ASTM Standard Designation: G119-93, "Standard Guide for Determining Synergism between Wear and Corrosion" ASTM Standards, vol. 3.02, (1993), p. 139.
25. D. Lopez, N.A. Falleiros, A.P. Tschiptschin, "Effect of nitrogen on the corrosion-erosion synergism in an austenitic stainless steel", *Tribol. Int.* 44, (2011), pp. 610-616.
26. S. Das, Y.L. Saraswathi, D.P. Mondal, "Erosive-corrosive wear of aluminum alloy composites: Influence of slurry composition and speed", *Wear* 261, (2006), pp. 180-190.